

RESEARCH

Open Access



Characteristics of cortical thickness in treated HIV-infected individuals with and without cognitive impairment

Ruili Li^{1,2†}, Guangxue Liu^{3†}, Xire Aili^{4,5}, Miao Zhang^{1,2}, Hongjun Li^{5*} and Jie Lu^{1,2*}

Abstract

Background HIV can alter the brain structure and function in the early stage of infection. This study investigated the differences in cortical thickness patterns between healthy controls (HCs) and people living with HIV (PLWH) with asymptomatic neurocognitive impairment (ANI) or cognitive integrity (CI).

Methods Twenty-one ANI, 25 CI, and 24 HCs were recruited and underwent high-resolution T1-weighted magnetic resonance images. Cortical thickness was analyzed using the Computational Anatomy Toolbox, and the correlation analysis was conducted between cortical thickness and clinical and neuropsychological variables.

Results Both CI and ANI exhibited decreased cortical thickness, primarily in the left frontal cortices and bilateral limbic system. ANI demonstrated a more pronounced and widespread pattern of cortical thinning. Lower CD4⁺ counts and higher peak plasma viral load were associated with decreased cortical thickness of the right pericallosal sulcus and middle-posterior part of cingulate gyrus and sulcus in ANI. Conversely, compared to HCs, both ANI and CI showed cortical thickening in the left insula cortex, and ANI tended to have a thicker cortex. Moreover, the increased thickness of left insula cortex in both CI and ANI were positively correlated with attention and working memory.

Conclusions The cortical thickness thinning was observed in the frontal and limbic systems in both ANI and CI. Meanwhile, the thickening of the insular cortex may represent mild neuroinflammation or a transient compensatory mechanism. This study provides new insights into the neural mechanisms underlying HIV-related cognitive impairment and highlights the importance of cortical thickness alteration patterns when assessing cognitive function of PLWH.

Keywords HIV-infection, Cognitive impairment, Cortical thickness, T1 weighted image, Magnetic resonance imaging

[†]Ruili Li and Guangxue Liu have contributed equally to this work.

*Correspondence:

Hongjun Li
lihongjun00113@ccmu.edu.cn

Jie Lu

lujie@xwhosp.org; imaginglu@hotmail.com

¹ Department of Radiology and Nuclear Medicine, Xuanwu Hospital, Capital Medical University, No.45 Changchun Street, Xicheng District, Beijing 100053, China

² Beijing Key Laboratory of Magnetic Resonance Imaging and Brain Informatics, Beijing 100053, China

³ Department of Natural Medicines, School of Pharmaceutical Sciences, Peking University Health Science Center, Beijing 100191, China

⁴ Beijing Advanced Innovation Center for Biomedical Engineering, Beihang University, Beijing 100191, China

⁵ Department of Radiology, Beijing Youan Hospital, Capital Medical University, No. 8 Xi Tou Tiao Youanmen Wai, Fengtai District, Beijing 100069, China



© The Author(s) 2025. **Open Access** This article is licensed under a Creative Commons Attribution-NonCommercial-NoDerivatives 4.0 International License, which permits any non-commercial use, sharing, distribution and reproduction in any medium or format, as long as you give appropriate credit to the original author(s) and the source, provide a link to the Creative Commons licence, and indicate if you modified the licensed material. You do not have permission under this licence to share adapted material derived from this article or parts of it. The images or other third party material in this article are included in the article's Creative Commons licence, unless indicated otherwise in a credit line to the material. If material is not included in the article's Creative Commons licence and your intended use is not permitted by statutory regulation or exceeds the permitted use, you will need to obtain permission directly from the copyright holder. To view a copy of this licence, visit <http://creativecommons.org/licenses/by-nc-nd/4.0/>.

Background

Studies have consistently shown that the human immunodeficiency virus (HIV) can invade the brain during early infection [1], leading to cognitive dysfunction [2]. Although combination antiretroviral therapy (cART) has successfully suppressed peripheral viral load, reduced the risk of major neurological complications, and improved cognitive function in people living with HIV (PLWH) over the long term, it has failed to effectively inhibit viral replication in central nervous system reservoirs [3], resulting in persistent cognitive impairments. Approximately 42.6% of PLWH are estimated to still suffer from HIV-associated neurocognitive disorders (HAND), with the mildest form of asymptomatic neurocognitive impairment (ANI), accounting for a substantial proportion of around 88% [4]. The accumulation of neurocognitive dysfunction over time, combined with increasing life expectancy, can result in adverse consequences such as poor medication compliance and a reduced quality of life [5]. Consequently, it is essential to focus greater attention on PLWH with ANI.

The underlying neurobiological mechanisms of HAND remain poorly understood, but non-invasive neuroimaging studies have consistently linked HAND to morphological changes in the brain [6–11]. After the introduction of potent cART, the phenotypic pattern of cognitive impairment in PLWH underwent a significant shift [7]. In the pre-cART era, subcortical regions and basal ganglia involvement were commonly implicated in cognitive impairment [6], whereas cortical involvement has been more frequently associated with impairment during the cART era [7]. Voxel-based morphometry (VBM) analysis is a valuable tool for localizing morphometric differences between groups [8–11]. Notably, VBM studies have revealed a marked decrease in cortical gray matter volume [8, 9], including the limbic lobe, cingulate gyrus, temporal cortex, superior/middle/inferior frontal gyrus, sub-lobar, and insula [10, 11].

The cerebral cortex, a hierarchical structure enveloping the brain, exhibits varying compositions and densities across its layers from inner to outer [12]. The segmented cerebral cortex can be investigated from three primary perspectives: surface area, folding patterns, and thickness [12]. In neuroanatomical research, cortical thickness measurements derived from surface-based morphometry (SBM) analyses are the most prevalent quantitative indices [12]. A key benefit of SBM lies in its ability to quantitatively assess absolute distances and shapes, thereby providing a more accurate representation compared to magnetic resonance imaging (MRI) intensity measurements [13]. Cortical thickness is formally defined as the distance between the gray-white border and the outer surface of the cortex. It can provide specific information

about neuronal loss or degeneration, as indicated by cortical thinning [14]. Investigations into cortical thickness have the potential to elucidate normal developmental and aging processes, as well as shed light on the precise morphological alterations associated with neurological disorders [12]. Consequently, employing SBM to investigate subtle alterations in gray matter structure may yield a clearer understanding of neuroanatomical changes in PLWH and offer deeper insights into the underlying mechanisms of HAND.

Some cross-sectional studies on untreated and treated cases and longitudinal studies following cART treatment have detected changes in cerebral cortex thickness [15–18]. Compared to healthy controls (HCs), PLWH who were largely treatment-naïve for cART showed significantly reduced cortical thickness in the right superior frontal gyrus [19]. PLWH who had largely received cART treatment showed cortical thinning in the primary somatosensory cortex, primary motor cortex, cingulate cortex, orbitofrontal cortex, and other frontal and temporal areas [17]. Additionally, PLWH who are on stable cART showed significant reduction in cortical thickness in multiple brain regions including the bilateral inferior temporal, para hippocampal, precentral, lateral occipital, right fusiform, insula and frontal regions, significant thicker cortex in the left isthmus cingulate and medial orbitofrontal regions [18]. In a one-year longitudinal follow-up study, no significant differences in cortical thickness were observed in PLWH with stable cART [20]. cART treatment-naïve PLWH exhibited poorer cognitive function and widespread cortical thinning in the primary motor cortex and temporal lobe than HCs. After starting cART, both brain structure and cognitive function showed improvement but remained lower than HCs over time [21]. There have been relatively few studies on the cortical thickness of PLWH in different cognitive states. In comparison to HCs, both HIV-infected individuals with cognitive integrity (CI) and HAND exhibited reduced cortical thickness, primarily in the bilateral primary sensorimotor cortex, extending to the prefrontal and parietal cortex. When directly compared to CI, HAND showed cortical alterations in certain areas, and a notable correlation was found between the thinning of the left retrosplenial cortex and cognitive functioning [22].

Despite existing reports on the effects of HIV infection and cART on cortical thickness, there remains a knowledge gap in understanding the alteration of cortical thickness in PLWH with different cognitive statuses, especially those with mildest cognitive dysfunction. The present study aimed to expand upon existing research by evaluating cortical thickness differences in ANI, CI and HCs, using the SBM analysis approach. Meanwhile, the correlations between cortical thickness differences and both

clinical variables and cognitive performance metrics were investigated further.

Materials and methods

Participants

In this clinical case–control study, a total of 51 PLWH were recruited from the infectious disease outpatient clinic of Beijing Youan Hospital, Capital Medical University. Meanwhile, 27 HCs were also recruited from the local community, and matched for age and gender with PLWH. The inclusion criteria for PLWH were as follows: right-handed, aged between 18 and 50 years, and diagnosed with HIV⁺ at the HAND preclinical stage. Similarly, the inclusion criteria for HCs were right-handed individuals between 18 and 50 years of age. The exclusion criteria for all participants were as follows: (1) alcohol or drug abuse; (2) a history of neurological or psychiatric diseases; (3) central nervous system infections (except HIV⁺) and tumors; (4) brain trauma; (5) cerebrovascular disease; (6) contraindication to MRI. The study was conducted in accordance with the Declaration of Helsinki, and was approved by the Institutional Review Boards of Beijing Youan Hospital, Capital Medical University, with Approval No.: [2023] 084, and Approval Date: August 24, 2023. Informed consent was obtained from all participants involved in the study.

The demographic information, including age, educational level, time since HIV⁺ diagnosis, nadir and current plasma CD4⁺ cell counts, CD4⁺/CD8⁺ ratio, and

peak plasma HIV RNA copies, were obtained from the patient’s self-reports and electronic medical records. The current laboratory examinations were conducted within 2–4 weeks of the MRI examination. Except for three participants who had taken cART for 1–3 months, all PLWH received stable cART for at least 6 months. The summary of demographic information and clinical laboratory test results is listed in Table 1.

Neuropsychological tests

Each participant is required to complete a comprehensive battery of neuropsychological tests 1–3 h before undergoing MR scan. These tests were designed to assess cognitive difficulties in daily life [23] and six cognitive domains [24]: verbal fluency, attention/working memory, executive function, learning and delayed recall, speed of information processing, and fine motor skills, as shown in Table 2. To minimize potential methodological differences or cultural bias in these cognitive assessments, a T-score for each test and participant was generated and adjusted for age, gender, and years of education. When a cognitive domain comprised multiple test scales, an averaged T-score was computed. The diagnosis of ANI was based on the following criteria: (1) performance in at least two domains was 1 standard deviation (SD) or more below the normative scores; (2) the cognitive impairment did not interfere with everyday functioning [25]. In this research, among the 51 HIV-infected subjects, 24 were

Table 1 Demographic, clinical variables, and neuropsychological data

| | ANI (n = 21) | CI (n = 25) | HCs (n = 24) | P values |
|--|------------------------|---------------------------|-----------------------|--------------------------|
| Gender (M/F) | 21/0 | 25/0 | 24/0 | N/A |
| Age (years) | 37.9 ± 7.4 | 37.6 ± 8.3 | 36.9 ± 7.9 | 0.910 ^a |
| Education level (years) | 14.0 (12 – 16) | 15.0 (13 – 16) | 15.5 (14 – 16) | 0.539 ^b |
| Time since HIV ⁺ diagnosis (months) | 50.4 (33.6 – 66.0) | 46.8 (20.4 – 85.2) | N/A | 0.791 ^c |
| Nadir CD4 ⁺ (cells/μl) | 335.0 (241.1 – 467.0) | 270.8 (172.0 – 445.2) | N/A | 0.574 ^c |
| Current CD4 ⁺ (cells/μl) | 480.0 (373.6 – 626.4) | 572.0 (448.0 – 766.9) | N/A | 0.408 ^c |
| Nadir CD4 ⁺ /CD8 ⁺ ratio | 0.26 (0.17 – 0.39) | 0.33 (0.21 – 0.49) | N/A | 0.774 ^c |
| Current CD4 ⁺ /CD8 ⁺ ratio | 0.68 (0.43 – 0.88) | 0.65 (0.42 – 0.79) | N/A | 0.708 ^c |
| Peak plasma viral load (copies/ml) | 31,872 (6827 – 77,841) | 31,546 (15,917 – 123,548) | N/A | 0.256 ^c |
| Current plasma viral load (copies/ml) | TND | TND | N/A | N/A |
| Scores of cognitive performances | | | | |
| Verbal fluency | 45.90 ± 10.70 | 55.46 ± 7.39 | 55.90 ± 4.67 | < 0.001 ^{a,***} |
| Attention/working memory | 35.36 ± 7.34 | 47.06 ± 7.40 | 47.50 ± 6.72 | < 0.001 ^{a,***} |
| Executive function | 45.99 ± 10.14 | 53.32 ± 7.05 | 53.71 ± 7.06 | 0.003 ^{a,**} |
| Learning and delayed recall | 39.64 ± 5.62 | 49.03 ± 6.46 | 49.40 (48.23 – 52.48) | < 0.001 ^{b,***} |
| Speed of information processing | 37.95 ± 12.09 | 47.76 ± 8.20 | 47.92 ± 10.12 | 0.002 ^{a,**} |
| Fine motor | 48.19 ± 9.76 | 45.80 ± 9.02 | 49.31 ± 10.50 | 0.442 ^a |

Normally distributed variables are listed with mean ± SD, while non-normally distributed variables are listed with median (IQR). ANI/PLWH with asymptomatic neurocognitive impairment, CI/PLWH with cognitive integrity, HCs healthy controls, M male, F, female, TND target not detected, N/A not available, ^aANOVA; ^bKruskal–Wallis test; ^cMann–Whitney U test; ^{*}P < 0.05; ^{**}P < 0.01; ^{***}P < 0.001. All tests were two-tailed

Table 2 Neuropsychological tests

| Cognitive domains | Neurocognitive scales |
|---|--|
| 1. Cognitive difficulties in daily life | A self-report by using a simple Activities of Daily Living scale questionnaire |
| 2. Cognitive domains | Corresponding neurocognitive scales |
| (1) Verbal fluency | Animal verbal fluency test (AFT) |
| (2) Attention/working memory | (1) Continuous performance test-identical pair (CPT-IP) |
| | (2) Wechsler memory scale (WMS-III) |
| | (3) Paced auditory serial addition test (PASAT) |
| (3) Executive function | Wisconsin card sorting tests (WCST-64) |
| (4) Learning and delayed recall | (1) Hopking verbal learning test (HVLTL-R) |
| | (2) Brief visuospatial memory test (BVM-T-R) |
| (5) Speed of information processing | Trail marking test A (TMT-A) |
| (6) Fine motor skills | Grooved pegboard |

diagnosed with ANI, and 27 were CI. All the cognitive tests of the HCs were normal.

Structural MRI acquisition

MRI examinations were performed using a Siemens 3 Tesla scanner (Tim-Trio, Siemens, Erlangen, Germany) with a 32-channel phased-array head coil. Two sequences were acquired: (1) axial T2-weighted fluid-attenuated inversion recovery (T2-FLAIR) with combined fat saturation to exclude visible intracranial lesion, with repetition time (TR) = 8000 ms, echo time (TE) = 97 ms, and inversion time (TI) = 2370.9 ms; (2) sagittal high-resolution 3D T1-weighted images (T1 WI) were acquired using magnetization-prepared rapid gradient echo (MPRAGE) with TR/TE/TI = 1900/2.52/900 ms, flip angle = 9°, acquisition matrix = 256 × 246, field of view = 250 × 250 mm², slice thickness = 1 mm, number of slices = 176, and 1 × 0.977 × 0.977 mm³ voxel size.

Image processing

A total of seven participants' scans (three ANI, two CI, and two HCs) were excluded from the final analyses due to poor image quality resulting from motion artifacts. The high-resolution T1 WI was processed using the Computational Anatomy Toolbox (CAT12) (<http://dbm.neuro.uni-jena.de/cat/>), which offers a fully automated approach to estimating cortical thickness based on the projection-based thickness method [14]. Briefly, the processing pipeline involved correcting bias fields, skull stripping, automating segmentation into gray matter, white matter, and cerebrospinal fluid, aligning images to the Montreal Neurological Institute (MNI) template space, and applying nonlinear deformations. For cortical thickness measurement, the workflow involves tissue segmentation to estimate the white matter distance. The local maxima, equivalent to the cortical thickness, were

then projected to other grey matter voxels using a neighbor relationship defined by the white matter distance. Finally, cortical thickness maps were smoothed using a 15 mm full width at half maximum of the Gaussian heat kernel. For quality control, all images were visually checked after the automated analyses, and all data passed.

Statistical analysis

Demographic and clinical variables

Statistical analyses were performed utilizing IBM SPSS Statistics for Windows, version 22.0 (IBM Corp., Armonk, N.Y., USA) for demographic, clinical characteristics, and neuropsychological variables. First, the Shapiro-Wilks test was used to check the normality of all continuous variables. The ages, education level and neuropsychologic test scores were evaluated using a one-way analysis of variance test (ANOVA) (for normally distributed variables), or the Kruskal–Wallis test (for non-normally distributed variables). The Mann–Whitney U test was used to assess the differences between the two HIV⁺ groups in terms of the time since HIV⁺ diagnosis, nadir and current plasma CD4⁺ cell counts, CD4⁺/CD8⁺ ratio, peak plasma viral load (non-normally distributed). Two-tailed statistical significance level was set at *P* < 0.05 for all tests.

Comparisons of cortical thickness

Subjects in the ANI, CI, and HCs groups were age and gender matched. ANOVA and post-hoc tests were conducted using vertex-wise analyses in each hemisphere to assess group differences in cortical thickness, with education level included as a covariate. Statistically significant voxels were obtained using SPM12, with a cluster-defining *P* value threshold of 0.001 for ANI vs HCs and CI vs HCs, and a *P* value threshold of 0.05 for ANI vs CI. Subsequently, the corrections for multiple

comparisons were conducted using the family-wise error (FWE) method with a corrected cluster significance of $P < 0.05$.

Correlation analysis

Correlations between cortical thickness and clinical variables, as well as neuropsychological test scores, were examined using Spearman correlation analysis, and the correlation coefficients (r) were calculated. The significance level was set at $P < 0.05$, two-tailed. After correlation analysis, Bonferroni correction was applied for multiple comparisons.

Results

Participant characterization

The demographic characteristics are presented in Table 2. There were no significant differences in gender, age or years of education among the ANI, CI, and HCs groups. For HIV⁺ groups (ANI and CI), no significant differences were found in the time since HIV⁺ diagnosis, nadir and current plasma CD4⁺ cell counts, CD4⁺/CD8⁺ ratio, and peak plasma viral load. In comparison to CI, ANI tended to have a longer disease course, lower current CD4⁺ cell counts, lower nadir CD4⁺/CD8⁺ ratio, and higher peak plasma viral load. As a result of cART, current plasma viral load was suppressed and undetectable in all PLWH. Notably, most cognitive scale scores in ANI group were lower than those in CI group, indicating that cognitive impairment persists despite plasma virus suppression in cART. Approximately 46% of the HIV-infected individuals were diagnosed with ANI. As shown in Table 1.

Alterations of brain cortical thickness based on vertex-wise analyses

The one-way ANOVA results showed significant differences in cortical thickness among the three groups, primarily involving the bilateral pericallosal sulcus (PeriCS) & middle-posterior part of the cingulate gyrus and sulcus (pMCC), the left superior frontal gyrus (SFG), orbital gyri (OG) & straight gyrus (SG), and the right paracentral lobule and sulcus (ParaCLS). In post-hoc analysis, compared to HCs, ANI exhibited reduced cortical thickness mainly in the bilateral PeriCS & pMCC, left SFG, OG & SG, and the right ParaCLS. Similarly, compared to HCs, CI showed reduced cortical thickness in the bilateral PeriCS & pMCC, left SFG, OG & SG ($P < 0.05$, FWE corrected). It is noteworthy that ANI presented a lower and broader trend of cortical thickness thinning. Furthermore, at a cluster-defining P values threshold of 0.001, there was no significant difference between ANI and CI. Finally, at a cluster defining P values threshold of 0.05, in direct comparison with CI, ANI had a greater cortical thickness in the left superior, inferior, and anterior segment of the circular sulcus of the insula (CSI) ($P < 0.05$, FWE corrected), whereas no regions exhibited thinner cortical thickness in ANI. As shown in Table 3, Figs. 1 and 2.

Correlation analysis

The association between cortical thickness and clinical variables revealed that cortical thickness values in the right PeriCS & pMCC in individuals with ANI were positively correlated with current CD4⁺ counts ($r = 0.517$, $P = 0.016$) and negatively correlated with peak plasma viral load ($r = -0.502$, $P = 0.02$). Additionally, cortical thickness values in the right ParaCLS in individuals with ANI were positively associated with nadir CD4⁺ counts ($r =$

Table 3 The comparisons of cortical thickness among ANI, CI, and HCs

| Comparison groups | Hemisphere | Overlap of atlas region | Cluster size (vertices) | Peak MNI coordinate | | | t values | P values (FWE) |
|-------------------|------------|-------------------------|-------------------------|---------------------|------|------|----------|----------------|
| | | | | X | Y | Z | | |
| HCs vs ANI | Left | PeriCS & pMCC | 229 | − 5 | − 8 | 31 | 12.0 | < 0.001 |
| | | SFG | 118 | − 6 | 52 | 39 | 8.0 | 0.013 |
| | | OG & SG | 101 | − 7 | 54 | − 24 | 8.2 | 0.028 |
| | Right | PeriCS & pMCC | 183 | 5 | − 7 | 33 | 6.8 | 0.001 |
| | | ParaCLS | 100 | 2 | − 30 | 70 | 6.6 | 0.030 |
| | | | | | | | | |
| HCs vs CI | Left | PeriCS & pMCC | 215 | − 5 | − 8 | 31 | 11.0 | < 0.001 |
| | | SFG | 94 | − 6 | 52 | 39 | 6.6 | 0.039 |
| | | OG & SG | 94 | − 7 | 54 | − 24 | 7.5 | 0.037 |
| | Right | PeriCS & pMCC | 159 | 3 | − 4 | 30 | 5.9 | 0.002 |
| | | | | | | | | |
| | | | | | | | | |
| ANI vs CI | Left | CSI | 904 | − 36 | − 14 | 13 | 2.8 | < 0.001 |

ANI PLWH with asymptomatic neurocognitive impairment, CI PLWH with cognitive integrity, HCs healthy controls, MNI Montreal Neurological Institute, FWE family-wise error, PeriCS pericallosal sulcus, pMCC middle-posterior part of the cingulate gyrus and sulcus, SFG superior frontal gyrus, OG orbital gyri, SG straight gyrus, ParaCLS paracentral lobule and sulcus, CSI circular sulcus of insula

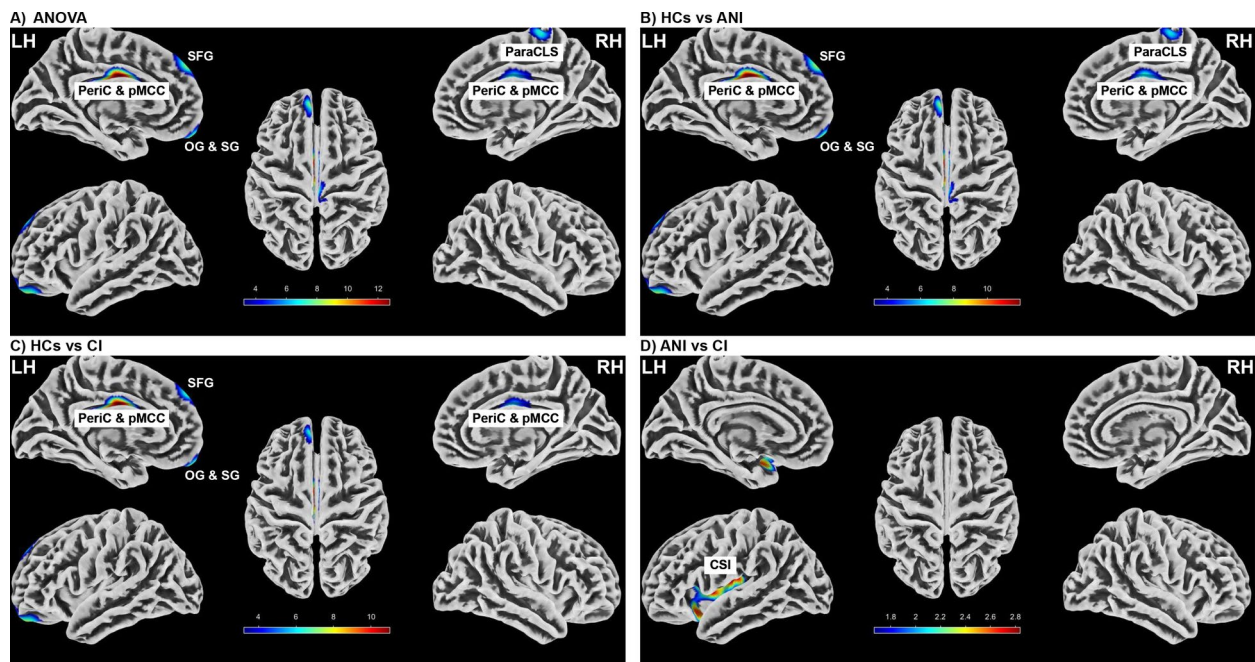


Fig. 1 Brain maps for cortical thickness differences of vertex-wise analyses from medial, lateral, and cranial views. **A** F-test revealed clusters of significant differences mainly located in the bilateral PeriCS & pMCC, the left SFG, OG & SG, and the right ParaCLS; **B** In comparison with HCs, cortical thickness was reduced mainly in the bilateral PeriCS & pMCC, left SFG, OG & SG, and the right ParaCLS of ANI patients; **C** CI group showed significantly smaller cortical thickness in the bilateral PeriCS & pMCC, left SFG, OG & SG; **D** Compared with CI, ANI showed significantly larger cortical thickness in the left CSI ($P < 0.05$, FWE corrected). The color bar represented t values. *LH* left hemisphere, *RH* right hemisphere, *ANI* PLWH with asymptomatic neurocognitive impairment, *CI* PLWH with cognitive integrity, *HCs* healthy controls, *PeriCS* pericallosal sulcus, *pMCC* middle-posterior part of the cingulate gyrus and sulcus, *SFG* superior frontal gyrus, *OG* orbital gyri, *SG* straight gyrus, *ParaCLS* paracentral lobule and sulcus, *CSI* circular sulcus of insula

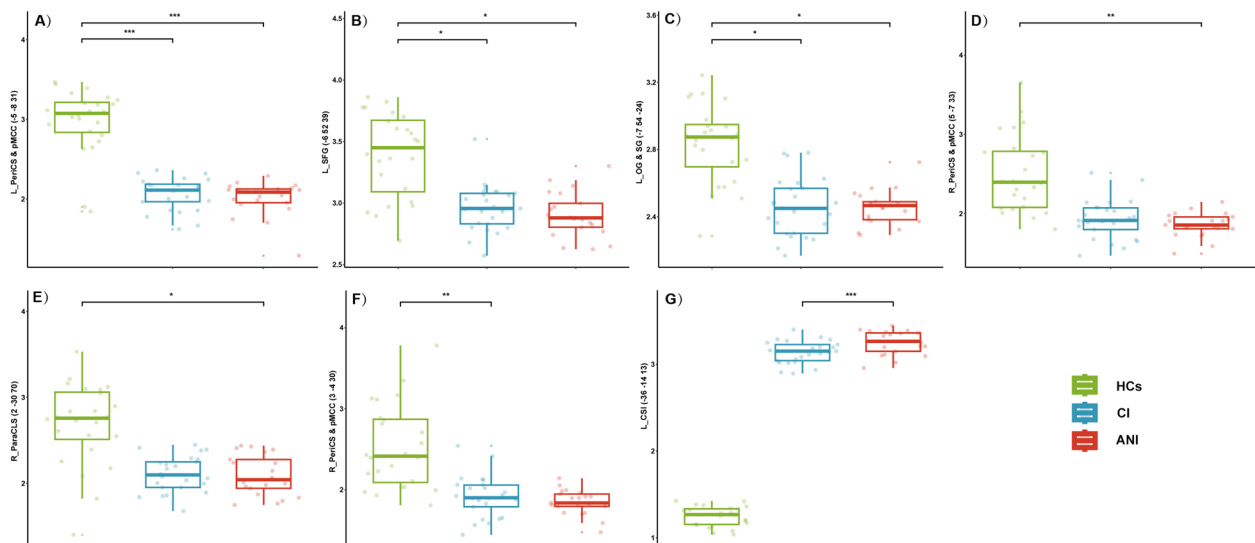
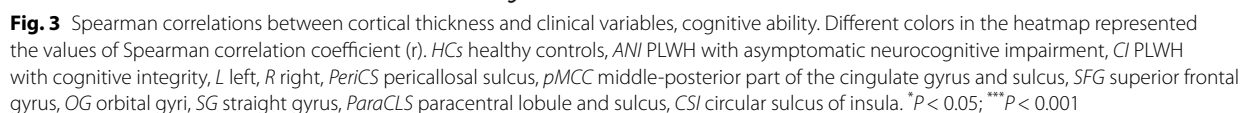


Fig. 2 Differences in cortical thickness of seven brain regions among HCs, CI, and ANI groups. Bar graphs presented the cortical thickness values. Compared with HCs, ANI and CI showed significant thinning in the cortical thickness of bilateral PeriCS & pMCC, left SFG, OG & SG, and right ParaCLS (with cluster-defining $P < 0.001$, FWE corrected $P < 0.05$). Although ANI and CI did not differ significantly in the above brain regions, ANI showed a tendency to lower cortical thickness. On the contrary, the cortical thickness of left CSI showed a gradual enlargement in the following order: HCs, CI, and ANI, (with cluster-defining $P < 0.05$, FWE corrected $P < 0.05$). *HCs* healthy controls, *ANI* PLWH with asymptomatic neurocognitive impairment, *CI* PLWH with cognitive integrity, *L* left, *R* right, *PeriCS* pericallosal sulcus, *pMCC* middle-posterior part of the cingulate gyrus and sulcus, *SFG* superior frontal gyrus, *OG* orbital gyri, *SG* straight gyrus, *ParaCLS* paracentral lobule and sulcus, *CSI* circular sulcus of insula. * $P < 0.05$; ** $P < 0.01$; *** $P < 0.001$

This research revealed a significant reduction in cortical thickness in the left SFG, OG, SG, the right ParaCLS, the bilateral PeriCS and pMCC in ANI group. The OG and SG are anatomical components of the inferior frontal gyrus, which is located within the orbitofrontal region. The inward part of extending precentral and postcentral gyrus is referred to as ParaCLS [26], involved in a variety of complex functions [27, 28]. The results of this study



confirmed previous observations [22, 29–33]. Thinning of the bilateral primary sensorimotor areas, prefrontal and parietal cortices were found in HAND [22]. Deformation-based morphometry analysis revealed deformation of gray matter in the bilateral SFG and the left middle frontal gyrus in PLWH [29]. Alterations in cortical thickness were basically synchronized with changes in whole brain volume. PLWH had significantly less gray matter in the medial frontal gyrus and SFG than HCs [30]. Autopsy pathology revealed a neuronal loss in the superior frontal gyrus [31] and calcarine cortex (primary visual area) [32] in PLWH. Synaptodendritic injury has been previously reported in the prefrontal cortex in PLWH [33]. Our results are also consistent with previous functional MRI studies [34, 35]. Local disruptions to the lateral magnetic field potential of the lateral prefrontal cortex were identified in PLWH using magnetoencephalography [34]. In a previous study, a decrease in resting-state functional MRI values was observed in the frontal/insular area of HAND [35]. The prefrontal cortex is functionally and anatomically connected by arcuate fibers and serves as a critical node integrating a variety of cognitive functions [36]. A significant positive correlation emerged between cortical thickness in the right ParaCLS and verbal fluency in ANI.

The PeriCS is a component of the limbic system, situated at the gray-white matter junction that separates the cingulate cortex from the limbic lobe [37]. Similarly, the pMCC is another component of the limbic system. Previous studies have documented volumetric alterations in the cingulate cortex when comparing PLWH to HCs [38]. The decreased NAA/Cr ratio in the pMCC observed in early-stage PLWH implies a direct neurotropism of the virus, leading to neuronal loss in this region [39, 40]. The pMCC serves as a critical hub for cognitive processing pathways, playing a pivotal role in memory, executive functioning [41], attention [41], and visual processing [42]. Damage to the cingulate cortex and its connections is associated with cognitive decline and reduced quality of life in PLWH [43, 44]. In our research, decreased current CD4⁺ counts and elevated peak plasma viral load were associated with a reduction in the cortical thickness of the right PeriCS & pMCC in individuals with ANI. These findings suggest that the PeriCS & pMCC may be especially susceptible to HIV-mediated neurotoxicity and that decreased current CD4⁺ counts could exacerbate the reduction of cortical thickness in these regions.

The relationship and interaction between the limbic system and prefrontal lobe is noteworthy. The limbic system primarily processes emotional experiences and forms memories, whereas the prefrontal cortex serves as the central hub for executive control and attentional modulation. Furthermore, the prefrontal cortex exerts a crucial regulatory influence over the limbic system.

They are not isolated from each other and have subtle connections that enable their functions to integrate. Functional MRI studies have found decreased functional connectivity between the frontal region and the precuneus, a region adjacent to the pMCC, in individuals with HAND compared to those with CI [45]. Additionally, altered intrinsic activity was observed in the frontal cortex but not in the pMCC [35]. These findings suggest that the frontal region may play a more critical role in disrupting functional connectivity between the limbic system and the prefrontal cortex.

In this study, PLWH with or without cognitive impairment exhibited significantly reduced cortical thickness in the frontal area and limbic systems compared to HCs. However, the cortical thickness in these regions failed to distinguish between ANI and CI, possibly due to the limited sample size. Despite the lack of differences in cortical thickness between the frontal area and limbic systems, individuals with ANI tended towards more widespread and thinner cortical involvement in these regions compared to those with CI, implying a potential contribution of these areas in the development of HAND in PLWH. The frontal lobe and limbic system may be susceptible to viral invasion, leading to gradual involvement and subsequent cognitive decline following HIV infection in the post-cART era. Neuroimaging techniques can detect these subtle, dynamic alterations. Further research is necessary to elucidate the underlying mechanisms driving these observations.

Moreover, individuals with ANI in our study showed significant impairments in verbal fluency, attention/working memory, executive function, learning, and delayed recall, as well as reduced speed of information processing compared to those with CI. Meanwhile, only fine motor skills were preserved in the ANI group. These findings are partially consistent with prior research [35]. The differences between our results and previous findings may be due to variations in the route of HIV transmission, severity of infection, cART treatment regimens, viral suppression, and CD4⁺ cell counts among different studies. Various confounding variables may have varying effects on cognitive function. The alterations in cortical thickness observed in the frontal lobe and limbic system may lead to clinically significant cognitive decline, which can be detected by neuropsychological assessments. Unexpectedly, in this study, the CI group also exhibited similar patterns of cortical thickness alterations as the ANI group. This suggests that subtle, clinically unrecognized alterations in cognitive processes may precede the diagnosis of HAND in PLWH, which can be detected using neuroimaging techniques. Future research is necessary to develop more cognitively demanding assessments

that can detect early alterations in cognitive function and elucidate their clinical implications for PLWH.

Interestingly, in contrast to the decrease in cortex thickness in the frontal cortex and other limbic systems, the insular cortex increases in thickness in both ANI and CI. Emerging evidence suggests that both the structure and function of the insula are altered among PLWH [46–49]. Children with HIV showed a thicker cortex compared to HIV-negative children in the left temporoinasular region. Children who experienced interrupted cART had a thicker cortex compared to HIV-negative controls in the right insular region. However, children receiving continuous cART did not show significant cortical thickness differences relative to controls [49]. The insula, a component of the limbic system, is known to play a crucial role in interoceptive processing, and emerging evidence suggests its involvement in emotional and cognitive processes [50]. Furthermore, the insula is characterized by bidirectional connections with critical cognitive regions, including the orbital prefrontal cortex and anterior cingulate cortex, and insular damage has been linked to cognitive impairments across various neuropsychological domains [50]. The clinical implications of these insular changes remain uncertain and warrant cautious interpretation. In our prior research, we observed that untreated PLWH with lower CD4⁺ exhibited diminished gray matter volume in the insula and heightened activation of both the insular and sensorimotor cortices when performing a hand movement task [48]. In this current investigation, all PLWH received treatment and were in the preclinical stage of HAND, during which the metabolic activity within the insula might intensify. Intense metabolic activity alongside persistent, mild neuroinflammation instigated by HIV viral proteins could potentially result in a transient thickening of the insular cortex. On the other hand, cognitive function might be transiently sustained by the brain's compensatory redistribution of other available reserve functions [51–53]. Recruitment of the additional insula region might be a compensatory mechanism for frontal damage and reduced efficiency, resembling a seesaw effect, which supports the compensation hypothesis. The orbitofrontal cortex is directly connected to the somatosensory cortex and integrates sensory information that supports higher-level cognition [54]. Consequently, the thinning of the prefrontal cortex may have disrupted the integration process, resulting in temporary excessive hyperplasia of the insular cortex. It is also worth noting that the degree of increase in insular cortex thickness with improved performance of attention/working memory was observed in both ANI and CI groups. These findings suggest that the degree of thickening in the insular cortex may serve as a valuable biomarker for cognitive impairment in PLWH.

This study has some limitations. First, the relatively limited sample size may compromise the generalizability of our findings. Second, this study is cross-sectionally designed, and all findings only show associations between cortical thickness and cognitive function, rather than causal relationships. Third, the lack of gender diversity in research samples, which consist solely of male participants, limits the generalizability of our findings to female populations. Nonetheless, our study offers valuable insights into the neural mechanisms underlying cognitive impairment in PLWH from a neuroimaging perspective. To further clarify these relationships, prospective longitudinal studies with larger, more diverse samples are necessary to validate and extend our findings.

Conclusions

In conclusion, this research provides novel neuroimaging evidence of cortical thickness alterations in PLWH. The altered cortical thickness in the frontal and limbic systems was consistently found in PLWH populations, regardless of their cognitive impairment status. Moreover, subjects in the ANI group tended to exhibit more pronounced cortical thickness alterations in these regions compared to those with CI. Additionally, an increase in the thickness of the insular cortex was observed, and it was positively correlated with attentional/working memory abilities. The increase in the insular cortex thickness may represent mild neuroinflammation or a transient compensation. As such, these regions may underlie the occurrence of cognitive impairment in PLWH during the cART era.

Abbreviations

| | |
|---------|---|
| HIV | Human immunodeficiency virus |
| PLWH | People living with HIV |
| ANI | PLWH with asymptomatic neurocognitive impairment |
| CI | PLWH with cognitive integrity |
| HCS | Healthy controls |
| HAND | HIV-associated neurocognitive disorders |
| cART | Combination antiretroviral therapy |
| MRI | Magnetic resonance imaging |
| SBM | Surface-based morphometry |
| MNI | Montreal Neurological Institute |
| T1 WI | T1-weighted images |
| ANOVA | Analysis of variance |
| FWE | Family-wise error |
| PeriCS | Pericallosal sulcus |
| pMCC | Middle-posterior part of the cingulate gyrus and sulcus |
| SFG | Superior frontal gyrus |
| OG | Orbital gyrus |
| SG | Straight gyrus |
| ParaCLS | Paracentral lobule and sulcus |
| CSI | Circular sulcus of insula |

Acknowledgements

Not applicable.

Author contributions

R.L.: designed research, performed research, collected data, analyzed data, and wrote paper; G.L.: performed research, analyzed data, and wrote paper; X.A.:

performed research, and collected data; M.Z.: performed research, and collected data; H.L.: designed research, performed research, and reviewed paper; J.L.: designed research, performed research, and reviewed paper. All authors read and approved the final manuscript.

Funding

Ruili Li and Hongjun Li disclose support for the research of this work from the National Natural Science Foundation of China (NSFC) [grant number 82202118 (R.L.), 61936013 (H.L.) and 82271963 (H.L.)]. The NSFC had no specific role in the conceptualization, design, data collection, analysis, decision to publish, or preparation of the manuscript.

Availability of data and materials

The datasets used and/or analysed during the current study are available from the corresponding author on reasonable request.

Declarations

Ethics approval and consent to participate

The study was conducted in accordance with the Declaration of Helsinki, and was approved by the Institutional Review Boards of Beijing Youan Hospital, Capital Medical University, with Approval No.: [2023] 084, and Approval Date: August 24, 2023. Informed consent was obtained from all participants involved in the study.

Consent for publication

Not applicable.

Competing interests

The authors declare no competing interests.

Received: 21 March 2025 Accepted: 4 April 2025

Published online: 15 April 2025

References

- Ragin AB, Wu Y, Gao Y, et al. Brain alterations within the first 100 days of HIV infection. *Ann Clin Transl Neurol*. 2015;2(1):12–21. <https://doi.org/10.1002/acn3.136>.
- Vance DE, Lee L, Munoz-Moreno JA, et al. Cognitive reserve over the lifespan: neurocognitive implications for aging with HIV. *J Assoc Nurses AIDS Care*. 2019;30(5):e109–21. <https://doi.org/10.1097/JNC.0000000000000007>.
- Gelman BB, Lisinichia JG, Morgello S, et al. Neurovirological correlation with HIV-associated neurocognitive disorders and encephalitis in a HAART-era cohort. *J Acquir Immune Defic Syndr*. 2013;62(5):487–95. <https://doi.org/10.1097/QAI.0b013e31827f1bdb>.
- Wang Y, Liu M, Lu Q, et al. Global prevalence and burden of HIV-associated neurocognitive disorder: a meta-analysis. *Neurology*. 2020;95(19):e2610–21. <https://doi.org/10.1212/WNL.00000000000010752>.
- Rojas-Celis V, Valiente-Echeverría F, Soto-Rifo R, Toro-Ascuy D. New challenges of HIV-1 infection: how HIV-1 attacks and resides in the central nervous system. *Cells*. 2019. <https://doi.org/10.3390/cells8101245>.
- Navia BA, Rostasy K. The AIDS dementia complex: clinical and basic neuroscience with implications for novel molecular therapies. *Neurotox Res*. 2005;8(1–2):3–24. <https://doi.org/10.1007/BF03033817>.
- Cysique LA, Brew BJ. Prevalence of non-confounded HIV-associated neurocognitive impairment in the context of plasma HIV RNA suppression. *J Neurovirol*. 2011;17(2):176–83. <https://doi.org/10.1007/s13365-011-0021-x>.
- Hoare J, Myer L, Heany S, et al. Cognition, structural brain changes, and systemic inflammation in adolescents living with HIV on antiretroviral therapy. *J Acquir Immune Defic Syndr*. 2020;84(1):114–21. <https://doi.org/10.1097/QAI.0000000000002314>.
- Cilliers K, Muller CJF. Effect of human immunodeficiency virus on the brain: a review. *Anat Rec (Hoboken)*. 2021;304(7):1389–99. <https://doi.org/10.1002/ar.24573>.
- Xu M, Ju XD. A meta-analysis of gray matter volume abnormalities in HIV patients. *Psychiatry Res Neuroimaging*. 2023;335: 111722. <https://doi.org/10.1016/j.pscychresns.2023.111722>.
- Kuper M, Rabe K, Esser S, et al. Structural gray and white matter changes in patients with HIV. *J Neurol*. 2011;258(6):1066–75. <https://doi.org/10.1007/s00415-010-5883-y>.
- Ay U, Kizilates-Evin G, Bayram A, Kurt E, Demiralp T. Comparison of FreeSurfer and CAT12 software in parcel-based cortical thickness calculations. *Brain Topogr*. 2022;35(5–6):572–82. <https://doi.org/10.1007/s10548-022-00919-8>.
- Canna A, Russo AG, Ponticorvo S, et al. Automated search of control points in surface-based morphometry. *Neuroimage*. 2018;176:56–70. <https://doi.org/10.1016/j.neuroimage.2018.04.035>.
- Dahnke R, Yotter RA, Gaser C. Cortical thickness and central surface estimation. *Neuroimage*. 2013;65:336–48. <https://doi.org/10.1016/j.neuroimage.2012.09.050>.
- Correa DG, Zimmermann N, Tukamoto G, et al. Longitudinal assessment of subcortical gray matter volume, cortical thickness, and white matter integrity in HIV-positive patients. *J Magn Reson Imaging*. 2016;44(5):1262–9. <https://doi.org/10.1002/jmri.25263>.
- du Plessis S, Vink M, Joska JA, et al. Prefrontal cortical thinning in HIV infection is associated with impaired striatal functioning. *J Neural Transm (Vienna)*. 2016;123(6):643–51. <https://doi.org/10.1007/s00702-016-1571-0>.
- Sanford R, Fernandez Cruz AL, Scott SC, et al. Regionally specific brain volumetric and cortical thickness changes in HIV-infected patients in the HAART era. *J Acquir Immune Defic Syndr*. 2017;74(5):563–70. <https://doi.org/10.1097/QAI.0000000000001294>.
- Joy A, Nagarajan R, Daar ES, et al. Alterations of gray and white matter volumes and cortical thickness in treated HIV-positive patients. *Magn Reson Imaging*. 2023;95:27–38. <https://doi.org/10.1016/j.mri.2022.10.006>.
- du Plessis S, Vink M, Joska JA, et al. Prefrontal cortical thinning in HIV infection is associated with impaired striatal functioning. *J Neural Transm*. 2016;123(6):643–51. <https://doi.org/10.1007/s00702-016-1571-0>.
- Corrêa DG, Zimmermann N, Tukamoto G, et al. Longitudinal assessment of subcortical gray matter volume, cortical thickness, and white matter integrity in HIV-positive patients. *J Magn Reson Imaging*. 2016;44(5):1262–9. <https://doi.org/10.1002/jmri.25263>.
- Weber MT, Finkelstein A, Uddin MN, et al. Longitudinal effects of combination antiretroviral therapy on cognition and neuroimaging biomarkers in treatment-naïve people with HIV. *Neurology*. 2022;99(10):E1045–55. <https://doi.org/10.1212/WNL.000000000000200829>.
- Shin NY, Hong J, Choi JY, Lee SK, Lim SM, Yoon U. Retrosplenial cortical thinning as a possible major contributor for cognitive impairment in HIV patients. *Eur Radiol*. 2017;27(11):4721–9. <https://doi.org/10.1007/s00330-017-4836-6>.
- Gandhi NS, Skolasky RL, Peters KB, et al. A comparison of performance-based measures of function in HIV-associated neurocognitive disorders. *J Neurovirol*. 2011;17(2):159–65. <https://doi.org/10.1007/s13365-011-0023-8>.
- Heaton RK, Clifford DB, Franklin DR, et al. HIV-associated neurocognitive disorders persist in the era of potent antiretroviral therapy CHARTER Study. *Neurology*. 2010;75(23):2087–96. <https://doi.org/10.1212/WNL.0b013e318200d727>.
- Antinori A, Arendt G, Becker JT, et al. Updated research nosology for HIV-associated neurocognitive disorders. *Neurology*. 2007;69(18):1789–99. <https://doi.org/10.1212/01.WNL.0000287431.88658.8b>.
- Jia H, Li Z, Guo F, et al. Cortical structure and the risk of amyotrophic lateral sclerosis: a bidirectional Mendelian randomization study. *Prog Neuropsychopharmacol Biol Psychiatry*. 2024;129: 110872. <https://doi.org/10.1016/j.pnpbp.2023.110872>.
- Sato W, Kochiyama T, Uono S, et al. The structural neural substrate of subjective happiness. *Sci Rep*. 2015;5:16891. <https://doi.org/10.1038/srep16891>.
- Cavanna AE, Trimble MR. The precuneus: a review of its functional anatomy and behavioural correlates. *Brain*. 2006;129(3):564–83. <https://doi.org/10.1093/brain/awl004>.
- Chen G, Cai DC, Song F, et al. Morphological changes of frontal areas in male individuals with HIV: a deformation-based morphometry analysis. *Front Neurol*. 2022;13: 909437. <https://doi.org/10.3389/fneur.2022.909437>.

30. Towgood KJ, Pitkanen M, Kulasegaram R, et al. Mapping the brain in younger and older asymptomatic HIV-1 men: frontal volume changes in the absence of other cortical or diffusion tensor abnormalities. *Cortex*. 2012;48(2):230–41. <https://doi.org/10.1016/j.cortex.2011.03.006>.
31. Everall IP, Luthert PJ, Lantos PL. Neuronal loss in the frontal cortex in HIV infection. *Lancet*. 1991;337(8750):1119–21. [https://doi.org/10.1016/0140-6736\(91\)92786-2](https://doi.org/10.1016/0140-6736(91)92786-2).
32. Everall IP, Luthert PJ, Lantos PL. Neuronal number and volume alterations in the neocortex of HIV infected individuals. *J Neurol Neurosurg Psychiatry*. 1993;56(5):481–6. <https://doi.org/10.1136/jnnp.56.5.481>.
33. Ellis R, Langford D, Masliah E. HIV and antiretroviral therapy in the brain: neuronal injury and repair. *Nat Rev Neurosci*. 2007;8(1):33–44. <https://doi.org/10.1038/nrn2040>.
34. Becker JT, Bajo R, Fabrizio M, et al. Functional connectivity measured with magnetoencephalography identifies persons with HIV disease. *Brain Imaging Behav*. 2012;6(3):366–73. <https://doi.org/10.1007/s11682-012-9149-4>.
35. Bak Y, Jun S, Choi JY, et al. Altered intrinsic local activity and cognitive dysfunction in HIV patients: a resting-state fMRI study. *PLoS ONE*. 2018;13(11): e0207146. <https://doi.org/10.1371/journal.pone.0207146>.
36. Li W, Qin W, Liu HG, et al. Subregions of the human superior frontal gyrus and their connections. *Neuroimage*. 2013;78:46–58. <https://doi.org/10.1016/j.neuroimage.2013.04.011>.
37. Vogt BA, Palomero-Gallagher N. Chapter 25—cingulate cortex. In: Mai JK, Paxinos G, editors. *The human nervous system*. 3rd ed. San Diego: Academic Press; 2012. p. 943–87.
38. Sanford R, Ances BM, Meyerhoff DJ, et al. Longitudinal trajectories of brain volume and cortical thickness in treated and untreated primary human immunodeficiency virus infection. *Clin Infect Dis*. 2018;67(11):1697–704. <https://doi.org/10.1093/cid/ciy362>.
39. Koltowska A, Hendrich B, Knysz B, et al. Analysis of metabolic changes of brain in HIV-1 seropositive patients with proton magnetic resonance spectroscopy. *Pol J Radiol*. 2010;75(2):27–32.
40. Boban JM, Kozic DB, Brkic SV, Lendak DF, Thurnher MM. Early introduction of cART reverses brain aging pattern in well-controlled HIV infection: a comparative MR spectroscopy study. *Front Aging Neurosci*. 2018;10:329. <https://doi.org/10.3389/fnagi.2018.00329>.
41. Leech R, Sharp DJ. The role of the posterior cingulate cortex in cognition and disease. *Brain*. 2014;137(1):12–32. <https://doi.org/10.1093/brain/awt162>.
42. Mohamed M, Barker PB, Skolasky RL, Sacktor N. 7T Brain MRS in HIV infection: correlation with cognitive impairment and performance on neuropsychological tests. *AJNR Am J Neuroradiol*. 2018;39(4):704–12. <https://doi.org/10.3174/ajnr.A5547>.
43. Wang B, Liu Z, Liu J, Tang Z, Li H, Tian J. Gray and white matter alterations in early HIV-infected patients: combined voxel-based morphometry and tract-based spatial statistics. *J Magn Reson Imaging*. 2016;43(6):1474–83. <https://doi.org/10.1002/jmri.25100>.
44. Strain JF, Cooley S, Kilgore C, et al. The structural and functional correlates of frailty in persons with human immunodeficiency virus. *Clin Infect Dis*. 2022;75(10):1740–6. <https://doi.org/10.1093/cid/ciac271>.
45. Ann HW, Jun S, Shin NY, et al. Characteristics of resting-state functional connectivity in HIV-associated neurocognitive disorder. *PLoS ONE*. 2016;11(4): e0153493. <https://doi.org/10.1371/journal.pone.0153493>.
46. Hammoud DA, Endres CJ, Hammond E, et al. Imaging serotonergic transmission with [¹¹C] DASB-PET in depressed and non-depressed patients infected with HIV. *Neuroimage*. 2010;49(3):2588–95. <https://doi.org/10.1016/j.neuroimage.2009.10.037>.
47. Schweinsburg BC, Scott JC, Schweinsburg AD, et al. Altered prefronto-striato-parietal network response to mental rotation in HIV. *J Neurovirol*. 2012;18(1):74–9. <https://doi.org/10.1007/s13365-011-0072-z>.
48. Zhou Y, Li R, Wang X, et al. Motor-related brain abnormalities in HIV-infected patients: a multimodal MRI study. *Neuroradiology*. 2017;59(11):1133–42. <https://doi.org/10.1007/s00234-017-1912-1>.
49. Nwosu EC, Holmes MJ, Cotton MF, et al. Cortical structural changes related to early antiretroviral therapy (ART) interruption in perinatally HIV-infected children at 5 years of age. *IBRO Neurosci Rep*. 2021;10:161–70. <https://doi.org/10.1016/j.ibneur.2021.02.001>.
50. Gasquoine PG. Contributions of the insula to cognition and emotion. *Neuropsychol Rev*. 2014;24(2):77–87. <https://doi.org/10.1007/s11065-014-9246-9>.
51. Contreras JA, Goni J, Risacher SL, Sporns O, Saykin AJ. The structural and functional connectome and prediction of risk for cognitive impairment in older adults. *Curr Behav Neurosci Rep*. 2015;2(4):234–45. <https://doi.org/10.1007/s40473-015-0056-z>.
52. Buckley R, Pascual-Leone A. Age-related cognitive decline is indicative of neuropathology. *Ann Neurol*. 2020;87(6):813–5. <https://doi.org/10.1002/ana.25733>.
53. Towe SL, Meade CS, Cloak CC, Bell RP, Baptiste J, Chang L. Reciprocal influences of HIV and cannabinoids on the brain and cognitive function. *J Neuroimmune Pharmacol*. 2020;15(4):765–79. <https://doi.org/10.1007/s11481-020-09921-y>.
54. Rolls ET. Convergence of sensory systems in the orbitofrontal cortex in primates and brain design for emotion. *Anat Rec A Discov Mol Cell Evol Biol*. 2004;281(1):1212–25. <https://doi.org/10.1002/ar.a.20126>.

Publisher's Note

Springer Nature remains neutral with regard to jurisdictional claims in published maps and institutional affiliations.